A13A-0210. Aircraft observations of convective characteristics throughout a Madden-Julian Oscillation event

N. Guy[1], D. P. Jorgensen[1], S. Chen[2], and Q. Wang[3]

[1] NOAA National Severe Storms Laboratory, Norman, OK, USA; [2] University of Miami, Miami, FL, USA; [3] Naval Postgraduate School, Monterey, CA, USA

Corresponding author email: Nick.Guy@noaa.gov

1. Introduction

A dominant component of intraseasonal (30-90 day) tropical variability is the MJO (Madden and Julian 1971, 1972). An MJO event is characterized by an eastward-moving envelope of deep convection (initiated over the equatorial Indian Ocean) and precipitation (usually comprised of multiple mesoscale convective systems) coupled to large-scale atmospheric circulations. The MJO has been shown to influence monsoon systems (e.g. Asia, Africa, Australia), tropical cyclones in all cyclone basins, midlatitude weather (e.g. rainfall and temperature variability), and other atmospheric and ocean phenomena (e.g. El Niño- Southern Oscillation, North Atlantic Oscillation, Indian Ocean Dipole); described in Lau and Waliser (2005) and Zhang (2005). Given the extensive impact of the MJO, it is important to correctly simulate the MJO in forecast and climate models. The Dynamics of the MJO (DYNAMO, 2011) field experiment obtained a large volume of data not typically available using in-situ and remote sensing techniques in this climatological MJO initiation region (Fig. 1). Expanding our understanding of convective dynamic and thermodynamic structure in this region is important to improve modeled MJO characteristics and forecast.

Figure 1. DYNAMO experiment location in reference to a world map.

3. Large-scale case synopsis

A strong MJO event occurred in late November (Fig. 3) corresponding to a convectively active time period within the observed domain. Three separate mission flights took place (22, 24, an 30 November) during this time, corresponding to MJO onset, active MJO, and a degrading MJO, respectively. Two RCE were modules performed during each mission. Strong MCSs were targeted in each case to ensure optimal data for dual-Doppler analyses (kinematic structure).

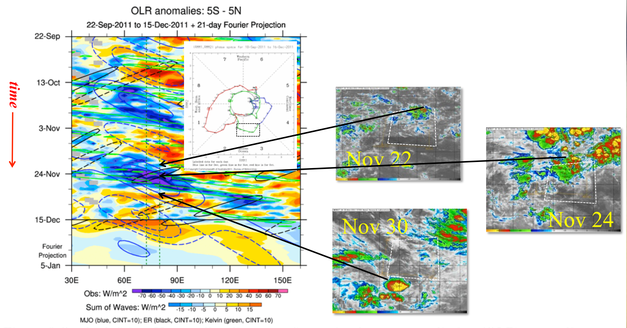

Figure 3.On the left is a Hovmoeller diagram of outgoing longwave radiation (OLR) anomalies (shaded) averaged from 5S–5N. Diagnosed wave events are noted with open contours and labeled in the bottom legend (image produced by Carl Schreck and available at http://monitor.cicsnc.org/mjo/dynamo_archive/2011-12-17/). Inlaid image shows an MJO phase diagram produced by the Australian Bureau of Meteorology. Images on the right are infrared satellite retrievals for in the region of interest showing the extent of convective activity.

5. Comparison of convective characteristics

While convection was present each day (Fig. 3), variability existed in the population of convective systems. Sampling individual storms provided insight into the 3D convective characteristics of systems which form the building blocks of the larger propagating convective envelope of the MJO.

Figure 5 helps summarize bulk distributions during the RCE modules in this study. While differences are observed in the distributions of horizontal maximum reflectivity composites, similarities in organization (largely due to the lack of strong wind shear) are apparent. Despite those similarities, echo top height composites indicated greater variability in the horizontal. Broadening of echo top height distributions phased with the MJO event evolution. This was influenced somewhat by the convective life cycle, where a larger population of building and decaying convection were present, acting to broaden the distribution. But besides heights were there differences in vertical structure between events?

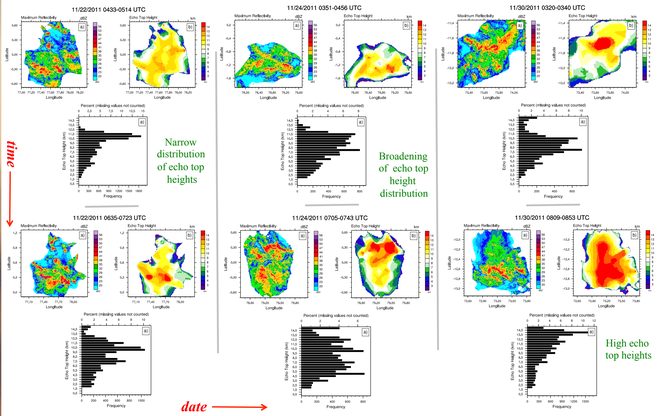

Figure 5. Each three panel plot displays composites of maximum radar reflectivity and maximum echo top height on top and a frequency distribution observed echo top height (frequency along abscissa). Date increases from left to right and time of day from top to bottom.

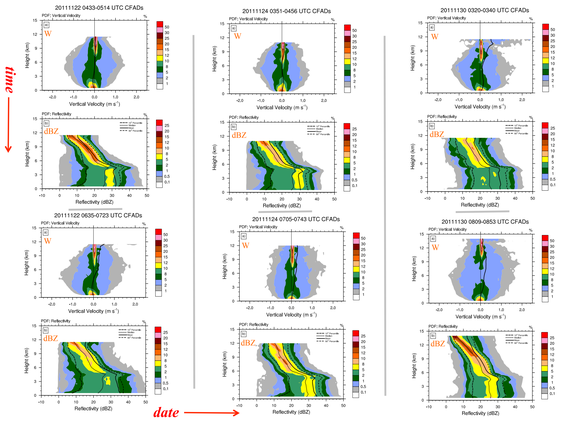

Figure 6. Each two panel plot displays CFAD diagrams of vertical velocity (top) and radar reflectivity (bottom). Solid lines are mean profiles in all plots. Additionally, 10th, 50th, and 90th percentiles are shown for reflectivity distributions. Date increases from left to right and time of day from top to bottom.

Contoured frequency-by-altitude diagrams (CFAD)s were used to analyse vertical distributions of vertical velocity and radar reflectivity. Downward motion was observed near the surface during the first mission (22 Nov), but was positive for 24 and 30 November where deep upward vertical motion was found. These deeper updrafts acted to loft hydrometeors to a higher altitude, thus broadening the reflectivity distributions aloft. Below the melting level (~4.5 km), distributions narrowed and developed a modal value near 30 dBZ, indicating consistent strong, widespread precipitation near the surface. The abundance of reflectivity values and upward vertical velocity values at high levels indicate the importance of ice microphysics during the initiation and peak phase of the MJO in this region.

2. NOAA P-3 aircraft platform

The NOAA P-3 aircraft conducted 12 flights from 11 Nov – 13 Dec 2011. This mobile platform offers a large number of measurements, including environmental state parameters (e.g. temperature, relative humidity), cloud and precipitation information (weather radar, liquid water content, particle probes), and sea surface temperature (via infrared retrieval). This study used data collected from a tail-mounted weather radar (characteristics shown in Table 1) and dropsondes (measuring vertical environmental thermodynamic profiles; time series shown in Fig. 4) to characterize mesoscale convective systems (MCSs).

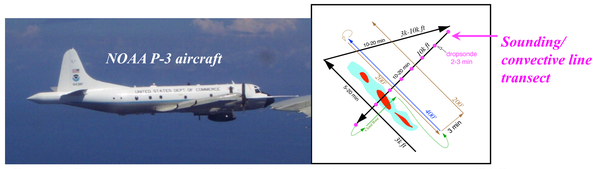

Figure 2. Flight pattern of the NOAA P-3 during radar convective element (RCE) modules designed to collect data during a convective event (convective system shaded).

Weather Radar Data and Methodology

Table 1. NOAA P-3 Doppler weather radar characteristics.

wavelength	3.22 cm (X-band)
PRF	3200/2400 s^{-1}
Unambiguous range	38 km
Nyquist velocity	±51 m s^{-1}
H beamwidth	1.35°
V beamwidth	1.90°
Pulse width	0.25/0.375 µs
Gate length	150 m
Antenna rotation	10 rpm (60° s^{-1})

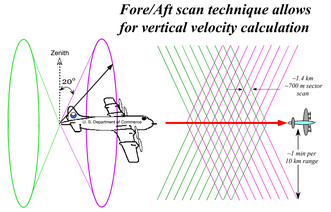

Sampling geometry of P-3 tail-mounted radar.

4. Convective environment structure

All events exhibited extensive stratiform precipitation and weakly organized convection on the mesoscale. While many convective bands were observed, a lesser degree of linearity was evident than previous oceanic field experiments, such as TOGA-COARE observations in the Western Pacific. Distinct cold pools were evident near the convectively active portion during the 22 and 24 November cases, with weak to no signal apparent on the 30 November (see A13A-0211 for more discussion). Generally increasing relative humidity was observed as the MJO event progressed. Figure 4 shows the horizontal extent and convective environmental characteristics along the flight leg transecting convective cells.

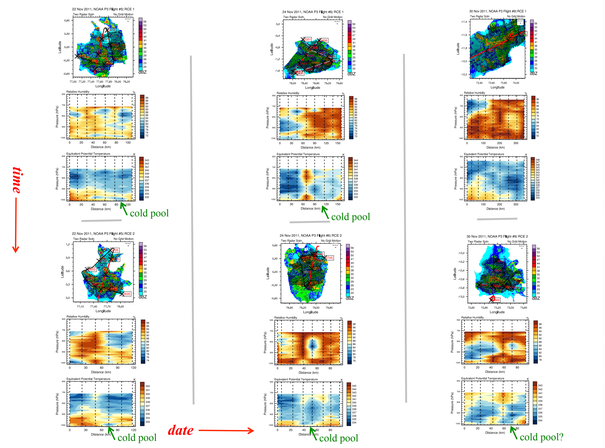

Figure 4. Three panel plots with a temporal/spatial composite of radar reflectivity, overlaid with dual-Doppler derived horizontal wind field and NOAA P-3 flight track (black line, with time [UTC] noted). The red portion of the flight track corresponds to the abscissa of the bottom two time series plots (relative humidity, and equivalent potential temperature) increasing by date from left to right and time of day from top to bottom. Vertical dashed lines represent the midpoint location of dropsonde descents.

6. Summary

- Airborne weather radar and dropsonde data were used to compare characteristics of convective systems in the Indian Ocean occurring during an MJO event.
- Similar attributes of the convective environment were observed during the MJO (e.g. cold pools, deep moisture profiles), with varying strength.
- Convective precipitation systems were found to display similar peak radar reflectivity values while having varying echo top heights.
- Echo top height distributions broadened as the MJO strengthened, followed by a narrowing.
- Deep updrafts loft hydrometeors to high levels, supporting the importance of ice microphysics in the maintenance of convection during the peak MJO.
- Correctly forecasting echo top height distributions of convection may be important to properly forecast the onset of an MJO.

7. Future work

- Comparison of these results and more to TOGA–COARE experiment results. The TOGA–COARE experiment took place in the Western Pacific, with many similar measurements for comparison.
- Calculate Z-R (radar reflectivity–rainfall) relationships for MJO and non-MJO events through analysis of airborne drop size distribution probes.
- Analysis of microphysics via cloud and precipitation probe measurements.
- Coordination with the TOGA and SMART-R radars on the R/V Revelle, which acquired data in coincident regions on the 22 and 24 Nov, 8 Dec, respectively.

References

Lau, W. K. M., and D. E. Waliser (2005), Intraseasonal Variability in the Atmosphere-Ocean Climate System. Springer, Chichester, UK, 477 pp.

Madden, R. A., and P. R. Julian (1971), Detection of a 40–50 day oscillation in the zonal wind in the tropical Pacific. *J. Atmos. Sci.*, 28, 702–708.

Madden, R. A., and P. R. Julian (1972), Description of global-scale circulation cells in the Tropics with a 40–50 day period. *J. Atmos. Sci.*, 29, 1109–1123.

Savarin, A., S. S. Chen, B. W. Kerns, C. Lee, and D. P. Jorgensen (2012), Convective Cold Pool Structure and Boundary Layer Recovery in DYNAMO. AGU Fall Meeting 2012, A13A-0211

Zhang, C. (2005), Madden-Julian oscillation. *Rev. Geophys.*, 43, 36 PP.

Acknowledgments. This research was undertaken as a National Research Council postdoctoral fellow and supported by a grant from the NOAA Climate Office (NA11OAR4310077).